MODELING THE CHARACTERISTICS OF A MAGNETICALLY SWITCHED PULSE-FORMING LINE*

D. M. Barrett
Lawrence Livermore National Laboratory
Livermore, California 94550

Abstract

Recent developments in magnetic switching technology have enabled linear induction accelerators to operate at high repetition rates. These accelerators provide high-average-power electron beams for many applications. However, some applications, such as free-electron lasers, also require a beam with a very narrow energy spread. As a result, the characteristics of the waveform driving the induction cell are very critical. Several accelerator systems at Lawrence Livermore National Laboratory use three-stage magnetic pulse compressors in which the final stage consists of a pulse-forming line (PFL) followed by a saturable output reactor. Ideally, the PFL forms a pulse with the required rise time and flatness. Unfortunately, traveling waves introduced on the PFL during the charging process as well as output switch performance may degrade the pulse shape.

To understand the effect of these factors upon the output pulse shape, we have used the computer code SPICE to model the final stage. The model simulates PFL dynamics under various conditions and includes a first-order model of the saturable output reactor. Discussed in this paper are the saturable inductor model and results obtained with the final stage compression model.

Introduction

Linear induction accelerators (LIAs) produce intense, high energy, pulsed electron beams for use in many applications.[1–3] Typical durations of these electron beam pulses are 60-80 ns. Such accelerators can deliver bursts of electron beam pulses occurring at multi-kilohertz repetition rates.

An LIA accelerates an electron beam passing through a series of ferrite-loaded induction cells. A voltage pulse driving each cell induces a changing flux within the ferrite material. The changing flux, in turn, induces an accelerating potential along the axis of the electron beam and increases its energy.

Induction cell drivers employed as magnetic pulse compression networks[4–6] enable LIAs to operate at high repetition rates. Unfortunately, these networks are often difficult to model, but models are essential for network design and optimization.

We have used the SPICE circuit code[7] to simulate the dynamics of the last stage of a three-stage magnetic compression network. We have developed a model to identify and optimize parameters important to the formation of the accelerator drive pulse. In this paper we describe the magnetic pulse compressor, the SPICE model, and results we obtained when modeling saturable-reactor output loss.

Magnetic Modulator Description

Figure 1 is a simplified circuit diagram of the MAG-1-D magnetic pulse compressor used at Lawrence Livermore National Laboratory. Capacitor C_1 is initially charged to 25 kV in about 3.8 μs, at which time L_1 saturates and allows C_1 to discharge into the primary of the 1:10 step-up transformer. L_1 has been designed to have a saturated inductance such that C_2 is charged to 250 kV in about 1 μs.

When C_2 is fully charged, L_2 saturates and begins to charge the 2-Ω, 35-ns, water-filled pulse-forming line (PFL). The charged PFL saturates L_3, whereupon the PFL is discharged into the load. The modeled portion of the network is enclosed within the dotted lines of Fig. 1. Specifically, the model simulates the dynamics of the PFL charging and then discharging into the load.

The output switch consists of a single-turn saturable reactor whose magnetic material consists of 0.6-mil-thick 2605CO Metglas. The flux

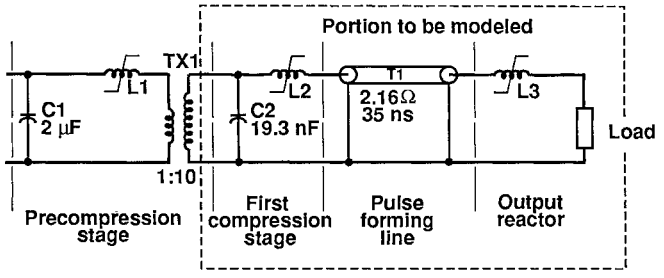

Figure 1. Simplified circuit diagram of the MAG-1-D magnetic pulse compressor.

swing of this material is approximately 3.2 T. The reactor core has an effective cross-sectional area and mean magnetic path length of 60 cm^2 and 95 cm, respectively.

Three physical characteristics of the output reactor must be represented as quantities suitable for the SPICE model. Specifically, these characteristics are the unsaturated inductance, the saturated inductance, and the volt-time product of the reactor. The unsaturated inductance, L_{unsat}, is calculated by using the core dimensions and estimating the relative permeability of the core based on the magnetization rate. Similarly, the saturated inductance, L_{sat}, is calculated from the core dimensions and allowing the saturated permeability of the core to be about 1.5 times the permeability of free space, u_0. Finally, the volt-time product, <vt>, of the core is calculated by

$$<vt> = NA\Delta B \ , \qquad (1)$$

where N is the number of turns on the reactor, A is the effective cross-sectional area of the reactor, and ΔB represents the flux swing of the reactor core. The calculated values of L_{unsat}, L_{sat}, and <vt> are 18.94 μH, 23.3 nH, and 22.06 mVs, respectively.

Circuit Model Description

Figure 2 shows the modeled first compression stage, PFL, and output reactor. Since the simulation begins with the discharge of C_2 into the PFL,

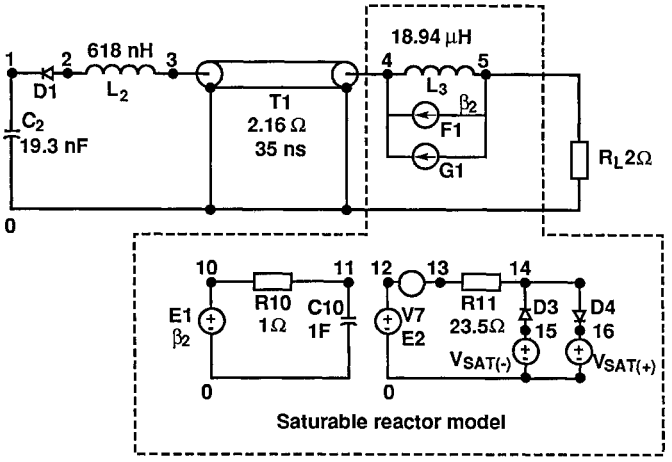

Figure 2. SPICE circuit model of the MAG-1-D pulse forming line and saturable output reactor.

* Work performed jointly under the auspices of the U.S. Department of Energy by LLNL under W-7405-ENG-48 and for the DOD under SDIO/ATC MIPR No. W31RPD-7-D4041.

Report Documentation Page

Form Approved
OMB No. 0704-0188

1. REPORT DATE	2. REPORT TYPE	3. DATES COVERED
JUN 1989	**N/A**	**-**

4. TITLE AND SUBTITLE
Modeling The Characteristics Of A Magnetically Switched Pulse-Forming Line

5a. CONTRACT NUMBER
5b. GRANT NUMBER
5c. PROGRAM ELEMENT NUMBER

6. AUTHOR(S)

5d. PROJECT NUMBER
5e. TASK NUMBER
5f. WORK UNIT NUMBER

7. PERFORMING ORGANIZATION NAME(S) AND ADDRESS(ES)
Lawrence Livermore National Laboratory Livermore, California 94550

8. PERFORMING ORGANIZATION REPORT NUMBER

9. SPONSORING/MONITORING AGENCY NAME(S) AND ADDRESS(ES)

10. SPONSOR/MONITOR'S ACRONYM(S)
11. SPONSOR/MONITOR'S REPORT NUMBER(S)

12. DISTRIBUTION/AVAILABILITY STATEMENT
Approved for public release, distribution unlimited

13. SUPPLEMENTARY NOTES
See also ADM002371. 2013 IEEE Pulsed Power Conference, Digest of Technical Papers 1976-2013, and Abstracts of the 2013 IEEE International Conference on Plasma Science. Held in San Francisco, CA on 16-21 June 2013. U.S. Government or Federal Purpose Rights License.

14. ABSTRACT
Recent developments in magnetic switching technology have enabled linear induction accelerators to operate at high repetition rates. These accelerators provide high-average-power electron beams for many applications. However, some applications, such as free-electron lasers, also require a beam with a very narrow energy spread. As a result, the characteristics of the waveform driving the induction cell are very critical. Several accelerator systems at Lawrence Livermore National Laboratory use three-stage magnetic pulse compressors in which the final stage consists of a pulse-forming line (PFL) followed by a saturable output reactor. Ideally, the PFL forms a pulse with the required rise time and flatness. Unfortunately, traveling waves introduced on the PFL during the charging process as well as output switch performance may degrade the pulse shape.

15. SUBJECT TERMS

16. SECURITY CLASSIFICATION OF:			17. LIMITATION OF ABSTRACT	18. NUMBER OF PAGES	19a. NAME OF RESPONSIBLE PERSON
a. REPORT	b. ABSTRACT	c. THIS PAGE			
unclassified	**unclassified**	**unclassified**	**SAR**	**4**	

we represent the first-stage compression reactor in its saturated state. In the actual circuit, after the PFL is fully charged, L_2 is forward saturated to prevent the PFL from discharging back into C_2. Therefore, diode D_1 has been included in the model to simulate this effect. The PFL is modeled as a 2.1-Ω, 35-ns, lossless transmission line.

The most challenging component to model was the saturable output reactor. Unfortunately, readily available versions of SPICE did not contain a nonlinear magnetic component model. However, several models have been developed for simulating nonlinear magnetic components for switching power supplies.[8] These models form the basis of the model we use to simulate output reactor operation.

The output reactor is modeled as an inductor, L_3, in parallel with a dependent current source, F_1. The inductor represents the unsaturated inductance of the reactor. Controlling the current flow through F_1 is a circuit that simulates the saturation dynamics of the reactor. The control circuit consists of an RC network (R_{10}, C_{10}) that integrates the voltage across the reactor model. The integrated voltage is proportional to the reactor flux and is subsequently shaped to represent the saturation dynamics of the reactor. The voltage source-diode combinations $V_{sat(+)}$-D_3 and $V_{sat(-)}$-D_4 simulate the positive and negative saturation fluxes, respectively. As long as the time integral of the voltage is between $V_{sat(+)}$ and $V_{sat(-)}$, both D_3 and D_4 are reverse biased, preventing any current flow through V_7. However, when the magnitude of the integral exceeds either $V_{sat(+)}$ or $V_{sat(-)}$, current flows through V_7 and controls current flowing through F_1. The value of R_{11} determines the current flowing through V_7, and, therefore, determines the saturated inductance of the reactor model.

We define several constants to make the model easier to implement. Before the voltage across the reactor model is integrated, it is multiplied by the constant $ß_1$. This correction is necessary because, without a multiplicative constant, the magnitude of the integral would be on the order of 30 mVs, which would produce about 30 mV at node 11. For the circuit to function as required, the voltage at node 11 must be significantly higher than the voltage drop across diodes D_3 and D_4. In addition, the constant $ß_2$ sets the ratio between the current flowing through V_7 and the saturated current flow through the main terminals of the reactor model.

The current supplied by F_1 can be expressed as

$$I_{F1}(t) = \frac{ß_1 ß_2}{R_{11}} \int V_{L3}\, dt - \frac{ß_2}{R_{11}} V_{sat} . \qquad (2)$$

The current flowing through an inductor as a function of the terminal voltage is given by

$$I_L(t) = \frac{1}{L} \int V_L\, dt . \qquad (3)$$

The first term of Eq. (2) can be rewritten as

$$\frac{ß_1 ß_2}{R_{11}} \int V_{L3}\, dt = \frac{1}{L_{sat}} \int V_{L3}\, dt ;$$

thus, the value of R_{11} is given by

$$R_{11} = ß_1 ß_2 L_{sat} . \qquad (4)$$

In this model, we choose $ß_1$ and $ß_2$ to be 10^6 and 10^3, respectively. As a result, R_{11} specifies L_{sat} in nanohenries. The values of $V_{sat(+)}$ and $V_{sat(-)}$ are related to the saturation flux as

$$\begin{aligned} V_{sat(+)} - V_{sat(-)} &= \langle vt \rangle \\ &= NA\Delta B \\ &= NA(B_{sat(+)} - B_{sat(-)}) , \end{aligned}$$

where $B_{sat(+)}$ and $B_{sat(-)}$ are the positive and negative values of B_{sat} (in mVs), respectively.

An initial-condition voltage on the integration capacitor, C_{10}, represents the reactor bias point. Typically, this inital voltage represents half the reactor volt-time product. As a result, the reactor is seen to be fully reset before the simulation begins.

Dynamic Loss Model

We modeled the dynamic loss by placing a voltage-dependent current source, G_1, across the terminals of the reactor model and by making the current flowing through G_1 a third-order polynomial function of the voltage across the reactor model terminals. Therefore, a nonlinear resistor is simulated. When a voltage is present across the reactor, power is dissipated by virtue of the current flowing through G_1. Since the voltage across the reactor is directly proportional to the magnetization rate, *dB/dt*, the amount of energy dissipated in the reactor while sustaining a voltage is also dependent on *dB/dt*.

By using a third-order polynomial to specify the leakage current, we can use available core loss data to simulate reactor loss. Several publications contain loss data for Metglas 2605CO[9,10] for magnetization rates of up to 10 T/μs, which is, unfortunately, much lower than the magnetization rate of the output reactor. Therefore, we estimate losses above 10 T/μs to be proportional to the square root of the magnetization rate. The loss, once ascertained, can be translated into a leakage current as a function of the voltage across the saturable reactor. We then use a curve-fitting routine to calculate the coefficients of the polynomial. For the loss to be independent of voltage polarity, the polynomial must be an odd function of voltage; i.e., $I_{G1}(v) = -I_{G1}(-v)$.

For this model, we set the coefficients of the polynomial at 0.0, 1.075×10^{-2}, 1.379×10^{-8} and -1.46×10^{-7}. Figure 3 shows the leakage current as a function of the voltage across the reactor model with these coefficients.

Reactor Model Test Circuit

To characterize the saturable reactor model, we modeled the test circuit of Fig. 4. With this circuit, the saturated inductance and the loss can be calculated and compared with expected results before the model is used with a more complex circuit. The test circuit consists of a capacitor initially charged to a voltage V_0. Then, capacitor voltage and current are monitored (Fig. 5) as the capacitor is discharged through the reactor. When the capacitor is first discharged, current flows through the reactor, setting the core to $+B_{sat}$ and reversing the voltage on the capacitor. The reversed capacitor voltage appears across the reactor until the <vt> of the reactor is exceeded, at which point saturation occurs and C_1 begins to discharge through the reactor once again. This process continues until the energy initially stored in C_1 has been dissipated.

One can calculate the saturated inductance of the modeled reactor by measuring the base width of the current pulse. For the case shown in Fig. 5, the base width was approximately 70 ns. Since the test circuit is a simple, very undamped LCR circuit, the saturated inductance is easily calculated as 24.3 nH. In addition, values for energy stored in the capacitor on each

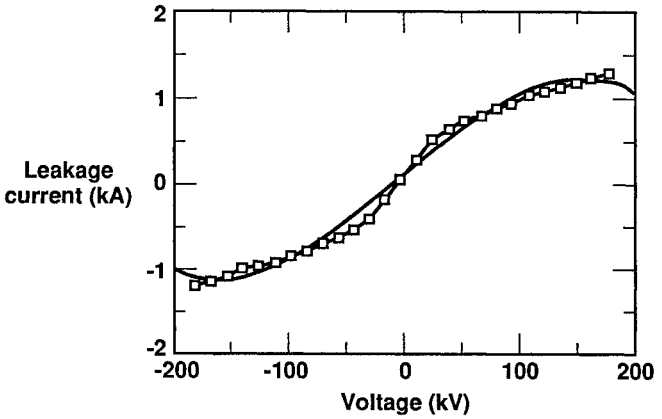

Figure 3. Estimated leakage current through the MAG-1-D output reactor as a function of voltage.

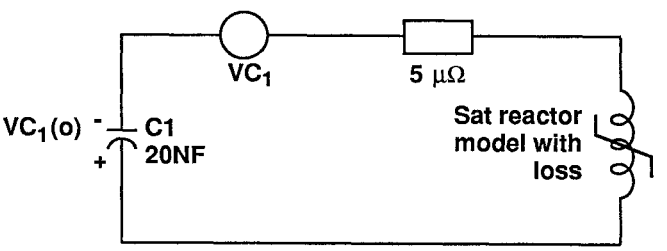

Figure 4. Test circuit used to measure the reactor model.

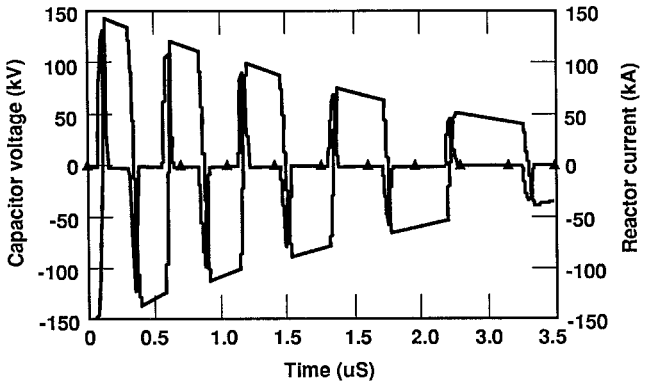

Figure 5. Voltage and current waveforms of the saturable reactor model in the test circuit.

successive voltage reversal can be used to calculate the energy loss over a range of *dB/dt* values. The energy loss as a function of *dB/dt* is shown in Fig. 6.

The test circuit can also be used to produce a B-H curve by plotting the voltage at node 11 [V(11)] as a function of $I(VC_1)$. V(11) is directly proportional to the reactor flux, *B*, and $I(VC_1)$ is directly proportional to the magnetization field, *H*. Scaling V(11) by the inverse of the effective cross-sectional area of the core yields a value for reactor flux in Teslas. Scaling $I(VC_1)$ by the inverse of the mean magnetic path length yields a magnetization field value in units of ampere-turns per meter. Figure 7 shows the B-H loop we calculated for the test reactor model.

Examples of Model Results

We used the SPICE model of the last section of the pulse compressor shown in Fig. 2 to predict the characteristics of the output pulse as the circuit parameters are varied. Model parameters that represent the present pulse compressor network are tabulated in Table 1.

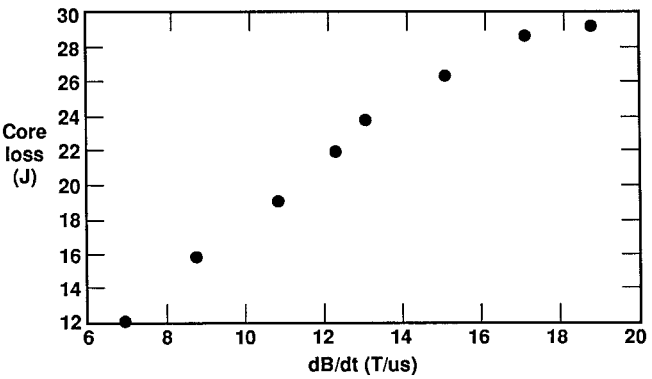

Figure 6. Loss of the saturable reactor model as a function of *dB/dt* obtained in the test circuit.

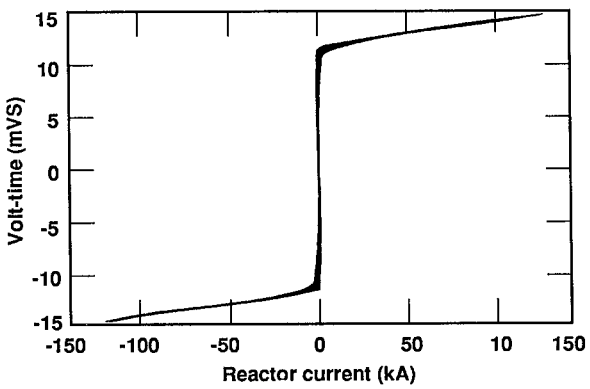

Figure 7. A B-H curve of the saturable reactor model. The volt-time axis is proportional to B. The reactor current axis is proportional to H.

Capacitor C_2 is initially charged to 250 kV. The results of the simulation are shown in Figs. 8 and 9. Reflections on the PFL distort the usual $(1 - \cos\omega t)$ charging waveform, as shown in Fig. 8. These reflections arise because the PFL charging period is not significantly longer than the PFL transit time. When the output reactor saturates, the PFL is discharged into the load, as shown in Fig. 9. The saturated inductance of the reactor model limits the output pulse rise time. Charging reflections cause the ripple riding on top of the pulse. These ripples can be minimized by varying L_2 slightly (which changes the PFL charge time) and discharging the PFL at the optimum time.

The simulation was repeated for three values of L_2 while <vt> was held constant at 22.06 mVs. The top portions of the output pulses are compared in Fig. 10. As can be seen, output flatness is a strong function of L_2. Increasing L_2 from 625 nH to 675 nH increases the charge time from 236 ns to 247 ns. Figure 11 shows the results of simulations for three values of <vt> while L_2 was held constant at 650 nH. Once again, the flatness of the output pulse is strongly influenced by the precise time at which the PFL discharges into the load.

Table 1. Correlation between circuit and model parameters.

Circuit parameters		Model parameters	
Component	**Value**	**Component**	**Value**
C_2	19.3 nF	C_2	19.3 nF
L_2 (sat)	650 nH	L_2	650 nH
T_1	2.1 Ω/35 ns	T_1	2.1 Ω/35 ns
L_3 (unsat)	18.94 μH	L_3	18.94 μH
L_3 (sat)	23.3 nH	R_{11}	23.3 Ω
L_3 (B_{sat})	−1.6 T	V_{sat} (+)	−11.03 V
L_3 (B_0)	1.6 T	V_{C10} (t = 0)	11.03 V

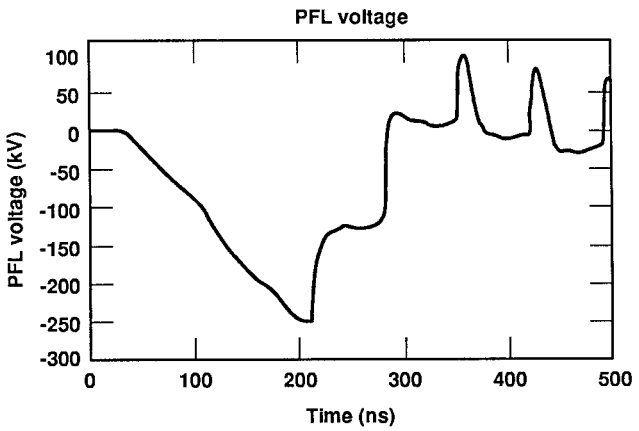

Figure 8. PFL voltage at output end.

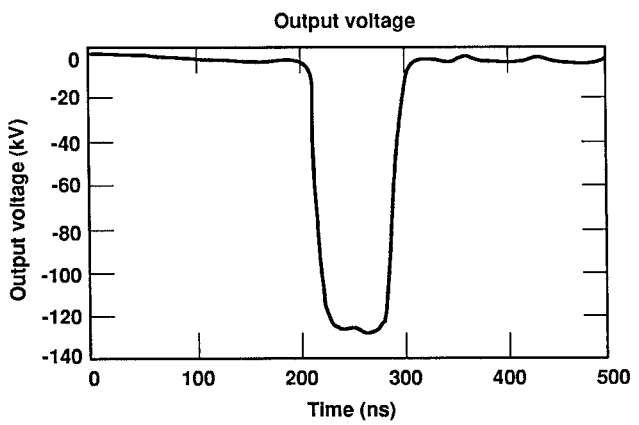

Figure 9. PFL output pulse across 2-Ω load.

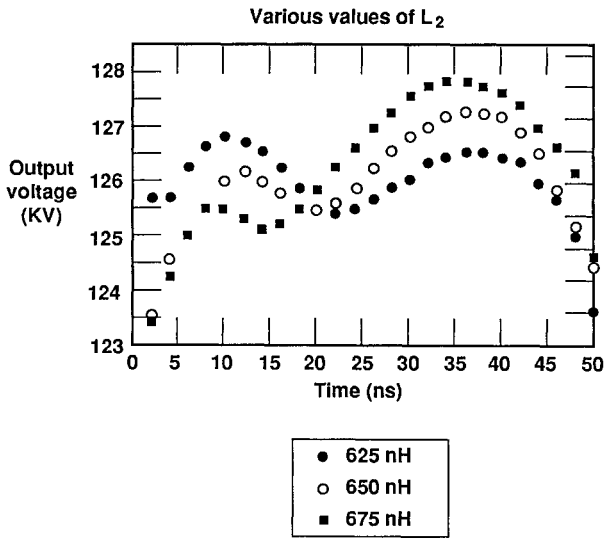

Figure 10. Magnitude of output voltage for various values of the PFL charging inductance L_2.

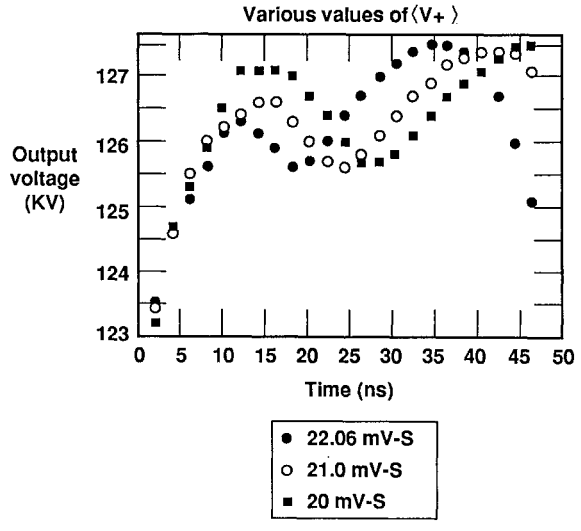

Figure 11. Magnitude of output voltage for various values of <vt>. The value <vt> is proportional to ΔB of the reactor core.

Conclusions

We have used the SPICE circuit simulation code to model the characteristics of a magnetically switched PFL. We modeled the output switch with a subcircuit that simulated the output reactor saturation properties. In addition, a simple loss model based on estimates of core loss at very high magnetization rates was used to simulate the loss characteristics of the reactor. The overall model has been useful in understanding how the shape of the output pulse is influenced by component values and other parameters.

References

[1] W. A. Barletta, "Accelerating Intense Electron Beams," in Energy and Technology Review, Lawrence Livermore National Laboratory, Livermore, Calif., UCRL-52000-79, September 1979.

[2] R. J. Briggs, D. L. Birx, D. S. Prono, D. Prosnitz, and L. L. Reginato, "Induction Linac Based FELs," in Proceedings of the IEEE Particle Accelerator Conference, Washington D.C., 1987, pp. 178 - 182.

[3] D. L Birx, S. A. Hawkins, S. E. Poor, L. L. Reginato, and M. W. Smith, "A Multi-Purpose 5-MeV Linear Induction Accelerator," in Proceedings of the IEEE Sixteenth Power Modulator Symposium, Arlington, Virginia, 1984, pp. 186-190.

[4] D. L. Birx, E. J. Lauer, L. L. Reginato, D. Rodgers Jr., M. W. Smith, and T. Zimmerman, "Experiments in Magnetic Switching," in Proceedings of the Third IEEE Pulsed Power Conference, Albuquerque, New Mexico, 1981, pp. 262 -268.

[5] C. H. Smith, "Metallic Glasses for Magnetic Switches," in Proceedings of the IEEE Fifteenth Power Modulator Symposium, Baltimore, Maryland, 1982, pp. 22 - 27.

[6] S. E. Ball and T. R. Burkes, "Saturable Inductors as High Power Switches," in Proceedings of the Third IEEE International Pulsed Power Conference, Albuquerque, New Mexico, 1981, pp. 269 - 272,

[7] SPICE is a general-purpose circuit simulation program developed by the Department of Electrical Engineering, University of California, Berkeley, Calif., 94720.

[8] P. Disheng and P. O. Lauritzen, "A Computer Model of Magnetic Saturation and Hysteresis for Use on SPICE2," IEEE Transactions on Power Electronics, vol. PE-1, No. 2, April 1986, pp. 101 -109.

[9] C. H. Smith and L. Barberi, "Dynamic Magnetization of Metallic Glasses," in Proceedings of the IEEE Fifth International Pulsed Power Conference, Arlington, Virginia, 1985, pp. 664 -667.

[10] C. H. Smith, "Permeabilities of Metallic Glasses at High Magnetization Rates," in Proceedings of the Eighteenth Power Modulator Symposium, Hilton Head, South Carolina, June, 1988, pp. 336 - 339.